Chemosphere 169 (2017) 403–412

Contents lists available at ScienceDirect

Chemosphere

journal homepage: www.elsevier.com/locate/chemosphere

Interactions among triphenyltin degradation, phospholipid synthesis and membrane characteristics of *Bacillus thuringiensis* in the presence of D-malic acid

Linlin Wang [a, b], Wenying Yi [a], Jinshao Ye [a, b, *], Huaming Qin [a], Yan Long [a], Meng Yang [a], Qusheng Li [a]

[a] Key Laboratory of Environmental Exposure and Health of Guangzhou City, School of Environment, Jinan University, Guangzhou, 510632, Guangdong, China
[b] Joint Genome Institute, Lawrence Berkeley National Laboratory, Walnut Creek, 94598, CA, USA

HIGHLIGHTS

- The accuracy of JC−1 use in *Bacillus thuringiensis* is verified.
- Spores in *B. thuringiensis* act as an indicator for MP and cellular activities.
- DMA at 1 mg L^{-1} promotes cellular metabolism increasing TPT degradation to 90%.
- DMA enhanced cellular and spore activity, and ion and phospholipid metabolism.
- Coexisting DMA and TPT depress FA synthesis but increase membrane permeability.

ARTICLE INFO

Article history:
Received 3 May 2016
Received in revised form
26 October 2016
Accepted 31 October 2016
Available online 23 November 2016

Handling Editor: Y Liu

Keywords:
Fatty acid
Transport
Membrane potential
Organotin
Organic acid

ABSTRACT

Degradation pathway and surface biosorption of triphenyltin (TPT) by effective microbes have been investigated in the past. However, unclear interactions among membrane components and TPT binding and transport are still obstacles to understanding TPT biotransformation. To reveal the mechanism involved, the phospholipid expression, membrane potential, cellular mechanism and molecular dynamics between TPT and fatty acids (FAs) during the TPT degradation process in the presence of D-malic acid (DMA) were studied. The results show that the degradation efficiency of 1 mg L^{-1} TPT by *Bacillus thuringiensis* (1 g L^{-1}) with 0.5 or 1 mg L^{-1} DMA reached values up to approximately 90% due to the promotion of element metabolism and cellular activity, and the depression of FA synthesis induced by DMA. The addition of DMA caused conversion of more linoleic acid into 10-oxo-12(Z)-octadecenoic acid, increased the membrane permeability, and alleviated the decrease in membrane potential, resulting in TPT transport and degradation. Fluorescence analysis reveals that the endospore of *B. thuringiensis* could act as an indicator for membrane potential and cellular activities. The current findings are advantageous for acceleration of biosorption, transport and removal of pollutants from natural environments.

1. Introduction

The global use of organotins has induced their widespread exposure in various ecosystems (Clarke and Smith, 2011; Fortibuoni et al., 2013). Triphenyltin (TPT), a representative organotin with endocrine behavior (Podratz et al., 2015), has resulted in worldwide contamination (Cole et al., 2015; Gui et al., 2016).

The reduction of phenyltins with thermal stability in a natural environment not exposed to ultraviolet radiation is primarily dependent on microbial communities. Therefore, selecting effective microbes, increasing degradation efficiency by adding exotic materials (Huang et al., 2014), and revealing TPT degradation pathways are of interest for researchers. Huang et al. (2014) had clarified that tea saponin significantly increased phenyltin solubility, biosorption and transport, and regulated cell metabolisms, such as improving protein expression, cell growth and ion use, accordingly stimulating phenyltin biodegradation. In addition, in a previous study,

* Corresponding author. Key Laboratory of Environmental Exposure and Health of Guangzhou City, School of Environment, Jinan University, Guangzhou, 510632, Guangdong, China.
E-mail addresses: jinshaoye@lbl.gov, folaye@126.com (J. Ye).

http://dx.doi.org/10.1016/j.chemosphere.2016.10.140
0045-6535/

the process of TPT adsorption and transport through cell walls and membranes was verified through molecular calculation and experiments (Tang et al., 2016). As a metabolic inhibitor (Fickova et al., 2015), TPT may depress cellular metabolism, including the synthesis of fatty acids (FAs), which are the main components of cell membranes. Whether this inhibition influences the interaction between membrane components and TPT transport is still unclear and needs to be revealed.

FAs are biomarkers for the evaluation of physicochemical activity and material transport under various stresses (Bernat and Dlugonski, 2012). Therefore, it is important to determine how TPT influences FA metabolism, and changes phospholipid components and structures by regulating related enzymes to resist environmental stresses; how FA changes further influence other metabolic pathways, such as ion metabolism, cell growth and apoptosis; and how this variation regulates FA metabolism.

Ten types of nutrients, including amino acids (L-threonine, L-asparagine, glutamic acid and glycine), organic acids (DMA, galacturonic acid and methyl pyruvate), a carbohydrate (D-cellobiose), an amine (putrescine) and an ester (tween40), were found to enhance the growth of *Bacillus thuringiensis*, a TPT degradation bacterium (Tang et al., 2016). TPT biodegradation is a metabolism-mediated process, some studies have tried to activate cellular metabolism involving organotin degradation through the addition of exotic materials (Huang et al., 2014; Tang et al., 2016). However, information regarding the influence of these nutrients on the TPT biodegradation mechanism is limited. Particular questions are how the nutrients interacted with TPT and FAs assisting TPT transport through the membrane and how they were used to influence FA synthesis and membrane potential (MP). It is thus vital to study the regulation of cellular metabolism, membrane composition, FA expression and MP in the presence of carbon nutrients during the TPT biodegradation process, which is of advantage for the acceleration of biosorption, transport and removal of pollutants from natural environments.

The relation between TPT degradation and 10 types of nutrients was investigated in this study. DMA was chosen for further studies due to its enhancement of TPT degradation. Cell surface element, FA metabolic pathway, spore fluorescence and MP were analyzed to determine cellular metabolic responses during the TPT degradation process by *B. thuringiensis* in the presence of DMA.

2. Materials and methods

2.1. Strain and chemicals

B. thuringiensis GIMCC1.817 was an effective microbe for TPT degradation (Tang et al., 2016) and was stored at the Microbiology Culture Centre of Guangdong Province, China. TPT was purchased from Sigma–Aldrich (St. Louis, MO, USA). Lysogeny broth (LB), a nutritionally rich medium primarily used for the growth of bacteria, was selected to culture *B. thuringiensis* in the current study, which contained 3 g L^{-1} beef extract, 10 g L^{-1} peptone and 5 g L^{-1} NaCl, individually. The concentrations of KH_2PO_4, NaCl, NH_4Cl and $MgSO_4$ in the mineral salt medium (MSM) were 30, 20, 30 and 10 mg L^{-1}, respectively. Extracellular K^+ and intracellular Na^+ regulate cellular Na^+/K^+-ATPase activities; NH_4^+ acts as a component of some biomolecules, like the N-terminal tail of peptidoglycans and proteins; Mg^{2+} is indispensable for enzymatic activity, metabolic regulation and nucleotide structural stability; PO_4^{3-} is involving in energy metabolism; and sulfur not only plays key roles in cell metabolism, but also acts as an essential structural constituent embedding in a great number of proteins (Wang et al., 2016). Therefore, these ions were used as the components of MSM for TPT degradation.

2.2. Biodegradation experiments

After 12 h of culture in LB medium at 30 °C and 130 r min^{-1}, *B. thuringiensis* was separated at 3500×*g* for 5 min and used to degrade 1 mg L^{-1} TPT. The biodegradation was performed at 130 r min^{-1} and 30 °C for 2 d in 20 mL of MSM with 0–20 mg L^{-1} L-threonine, L-asparagine, glutamic acid, glycine, DMA, galacturonic acid, methyl pyruvate, D-cellobiose, putrescine and tween40, respectively. After biodegradation, the total residual TPT was analyzed to determine the biodegradation efficiency (Huang et al., 2014). The residual DMA and some ions in the MSM medium were evaluated. Briefly, the solutions were centrifuged at 3500×*g* for 10 min. The concentrations of DMA, Cl^-, SO_4^{2-} and PO_4^{3-} in the supernatant were detected using an ICS–2500 ion chromatography system (Dionex, Sunnyvale, USA). OD_{600nm} and pH values of each sample before and after TPT degradation were also determined.

2.3. Cellular surface element change

The energy spectra of the control cells and those after TPT degradation with or without 1 mg L^{-1} DMA were detected using a scanning electron microscope (SEM; JSM–7001F) equipped with an energy-dispersive X-ray fluorescence spectrometer (QX200). To observe the actual cell status, samples without preliminary fixation were filtered using a 0.22-μm polyether sulfone filter and freeze-dried before SEM detection.

2.4. FA analysis

The species and content of FAs in the control cells and samples after TPT degradation with or without 1 mg L^{-1} DMA were analyzed. Briefly, 2 mL of methyl alcohol containing 2% H_2SO_4 were added to each sample. Subsequently, the sample tubes were filled with nitrogen. All samples were heated in an 80 °C water bath for 1 h. After cooling the samples to room temperature, 4 mL of a mixture of n-hexane and pure water (1:1, V/V) were added, and then the samples were vortexed. The organic portion was collected, dried by nitrogen, and concentrated with 1 mL of chromatographic class n-hexane containing 5 μL of methyl nonadecanoate for analysis. Parallel samples freeze-dried directly were prepared for quantification by measuring cell mass.

FAs were detected by gas chromatography-mass spectrometry (Shimadzu, Japan) using electronic ionization (70 eV) in scan mode (50–500 *m/z*) with a DB–5MS capillary column (30 m × 0.25 mm × 0.25 μm). Splitless injection of 1 μL of a sample was carried out with an autosampler. Helium was used as the carrier gas at a flow rate of 1 mL min^{-1}. The ion source and interface temperatures were set to 230 and 250 °C, respectively.

2.5. MP analysis

The control cells and those after TPT degradation with or without 1 mg L^{-1} DMA were harvested and suspended in 200 μL of 5,5',6,6'-tetrachloro-1,1'3,3'-tetraethylbenzimidazolcarbocyanine iodide (JC–1) to obtain a cell concentration of approximately 10^6 cells per milliliter. Subsequently, samples were placed in the dark at 37 °C for 15 min and analyzed using flow cytometry (FCM) to measure the MP.

FCM analysis was performed on a FACSAria flow cytometer (BD, USA) with 10,000 cells being acquired per sample at a flow rate of 10 μL min^{-1}. Green fluorescence (from JC–1 monomers; FL–1) and red fluorescence (from JC–1 aggregates; FL–2) were captured through 527 and 590 nm long-pass filters, respectively. Fluorescence data of cells stained with JC–1 were recorded by confocal laser scanning microscopy (CLSM; Zeiss, Germany) and analyzed by

FACSDiva (BD, USA).

2.6. Computational methods

To further determine the interaction between TPT and FAs with or without DMA, the three-dimensional structures of these compounds were created using ChemBio3D Ultra version 15.0. Subsequently, the energy of these structures was minimized by molecular mechanics until the root-mean-square gradient became smaller than 0.01 kcal mol^{-1} Å. The interaction between TPT and FAs with or without DMA was calculated by molecular dynamics. The step interval, frame interval and termination point of the calculation were 2 fs, 10 fs and 10,000 steps, respectively.

The biosynthesis of FAs and metabolism of cell membrane phospholipids were analyzed by KEGG Pathway (http://www.genome.jp/kegg/pathway.html) combined with the whole genome sequencing of *B. thuringiensis*.

2.7. Statistical analysis

All of the experiments were performed in triplicate, and the mean values were used in the calculations. MP was calculated by analysis of variance (ANOVA).

3. Results and discussion

3.1. TPT biodegradation with different carbon nutrients

Fig. 1a shows that amino acids, especially glycine but not glutamic acid at 0.5 and 1 mg L^{-1}, at low concentrations depressed TPT biodegradation. The influence of pH on TPT degradation was not obvious here (Figs. S1a–d). Based on the mineral absorption pathway (http://www.kegg.jp/kegg-bin/show_pathway?map04978), additional glycine tends to inhibit mineral absorption, which might be partially responsible for the decrease in TPT degradation. Regarding glutamic acid, it has been reported that this compound dissolved copper efficiently and enhanced its biosorption by heterotrophic bacteria (Kostudis et al., 2015). This characteristic of glutamic acid could also increase the solubility and utilization of TPT (Graceli et al., 2013).

Exotic organic acids such as galacturonic acid significantly reduced TPT degradation efficiency (Fig. 1b), which might be a result of the inhibiting effect of excessive H^+ on cell metabolism and H^+ adsorption on the cell membrane (Fig. S1e). On the other hand, cells tend to utilize easily transported and degraded nutrients rather than xenobiotics. The recovery of pH in high galacturonic acid concentrations was consistent with it. Galacturonic acid was one of those nutrients that could be easily used with the expression of a galacturonic acid transporter and an intracellular metabolism enzyme (Niu et al., 2015) leading to low TPT degradation rate. However, 0.5 and 1 mg L^{-1} DMA dramatically promotes TPT biodegradation, which might be primarily attributed to its biological functions, such as regulating FA synthesis and degradation by H^+ and NADPH metabolism (Fig. 2a), and relating to glyoxylate and dicarboxylate metabolism, pyruvate metabolism and citrate cycle (http://www.kegg.jp).

Fig. 1c illustrates that the effect of D-cellobiose and tween40 at different concentrations on TPT biodegradation was not obvious, while amine (putrescine) at concentrations above 3 mg L^{-1} decreased TPT biodegradation. According to its degradation pathway, putrescine was successively transformed to 4-aminobutyraldehyde, 4-aminobutyrate and succinate by the catalysis of putrescine specific amine oxidases accompanied with 4-aminobutyraldehyde dehydrogenase (Fostera et al., 2013). Therefore, the pH value in the medium would recover in some degreed. Fig. S1i showed that pH values recovered to neutral which means that cells tended to use putrescine instead of TPT.

3.2. The effect of DMA on cell metabolism

DMA in the studied concentrations effectively enhanced TPT biodegradation. Therefore, DMA was chosen for further studies.

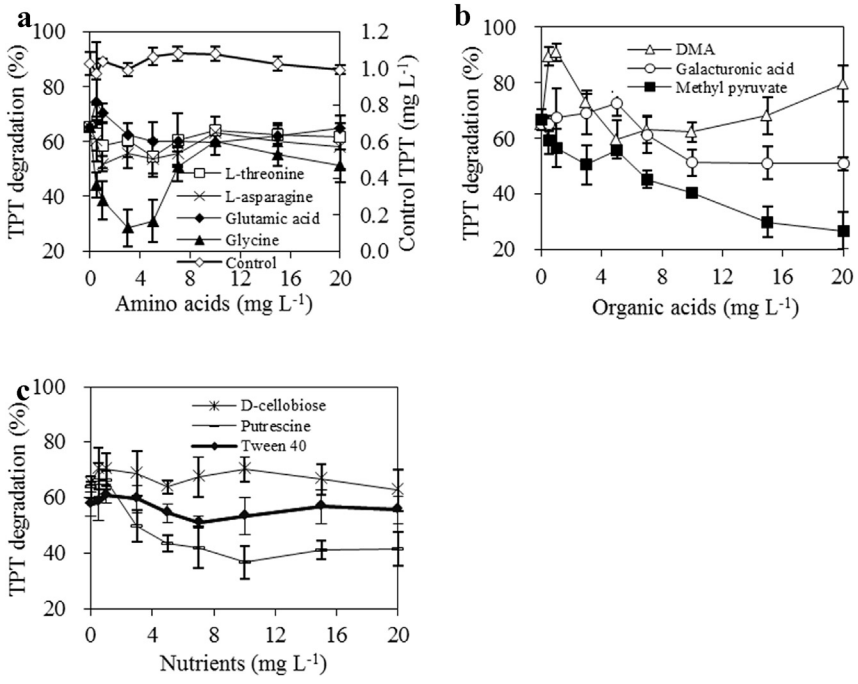

Fig. 1. Relation between carbon nutrients and TPT degradation. a: amino acids; b: organic acids; c: D-cellobiose, tween40 and putrescine.

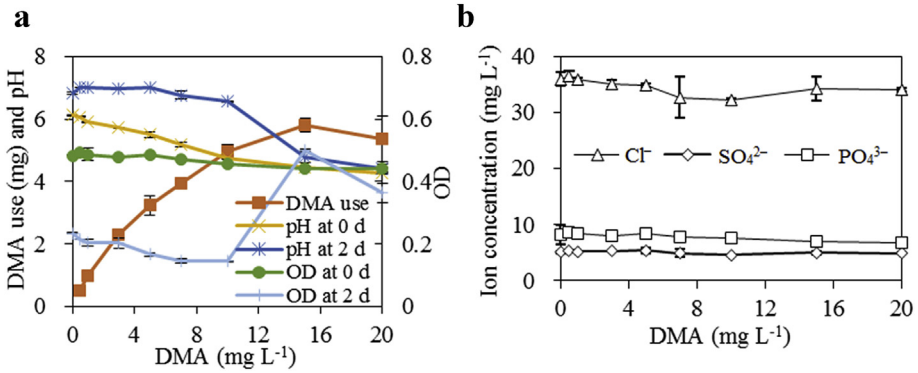

Fig. 2. The effect of DMA on cell metabolism. a: DMA use, pH and OD values; b: ion concentrations in MSM at 2 d.

Fig. 2a shows a gradually increasing DMA use when DMA in the concentration from 0.5 to 16 mg L^{-1}. However, the use of DMA at 20 mg L^{-1} decreased because of the inhibiting effect induced by high concentrations of H^+ and the fierce competition among the cells at high biomass dosages for nutrients. Biomass in MSM with 16 mg L^{-1} DMA after 2 d higher than that of 0 d was consistent with this inference. When the DMA concentration in the medium was high, cells tended to use DMA rather than TPT, which caused relatively low TPT degradation efficiency in this condition (Fig. 1b).

After 2 d of degradation, the pH in the medium with low concentrations of DMA was neutral, which was related to the regulation of H^+ metabolism by malic enzymes (Fig. 2a), whose activity could decrease the flux of pentose phosphate pathway, affect the ratios of redox cofactors, and then aerobically increase NADPH production to reduce H^+ in the medium (dos Santos et al., 2004). However, the pH of MSM with high concentrations of DMA in 2 d was not neutral, which implies that cell metabolism was significantly depressed in this condition. This is why TPT biodegradation efficiency and DMA use in high DMA concentrations were low. Furthermore, high levels of protons would compete with TPT to occupy cell surface binding sites, depress TPT biosorption, and thus reduce TPT biodegradation (Ye et al., 2013).

The effect of different concentrations of DMA on anion metabolism (Fig. 2b) was not distinct, which indicates that DMA at the studied concentrations did not significantly influence ion transport. Compared with their initial concentrations, the decreased values of Cl^-, SO_4^{2-} and PO_4^{3-} in MSM at 2 d illustrate that cells assimilated these ions during TPT degradation. Except for a concentration gradient, SO_4^{2-} and PO_4^{3-} assimilation was primarily due to cellular metabolism. TPT transport and degradation required PO_4^{3-}-containing polymers to provide energy and SO_4^{2-} to form sulfur-containing molecules, such as proteins.

3.3. Cell surface element analysis

To further illustrate the results on ion metabolism (Fig. 2b), energy-dispersive X-ray fluorescence spectroscopy was used to analyze the variation of cellular elements after TPT degradation in the presence of DMA at 1 mg L^{-1}. The major elements of each sample were sulfur, carbon and oxygen, which are essential elements for organisms. Nitrogen, phosphorus and potassium were detected on the surface of the control cells in the MSM without TPT and DMA at 0 d (Fig. 3a). Cells tend to metabolize nitrogen to form proteins, assimilate phosphorus to maintain energy metabolism and transport potassium by Na^+/K^+ pump to hold MP. However, cells prefer to deactivate ion transporters under sudden stress resulting in the decrease of elements detected. For example, concentrations of the three elements reduced immediately when cells were in contact with TPT or DMA (Fig. 3a). Chlorine was detected on the surface of the cells in contact with DMA, which means that the inhibiting effect of DMA for ion transports in 0 d was smaller than that of TPT. The study performed by Zdravkovic et al. (2012) had revealed that Cl^- was crucial to transport by prepping the active site of enzymes in membrane for subsequent ion or substrate binding, and further Cl^- binding translated to proper positioning, forming the most energetically favorable ion or substrate binding. Thus DMA might enhance TPT degradation by increasing TPT absorption on membrane proteins. Element metabolism of cells in the

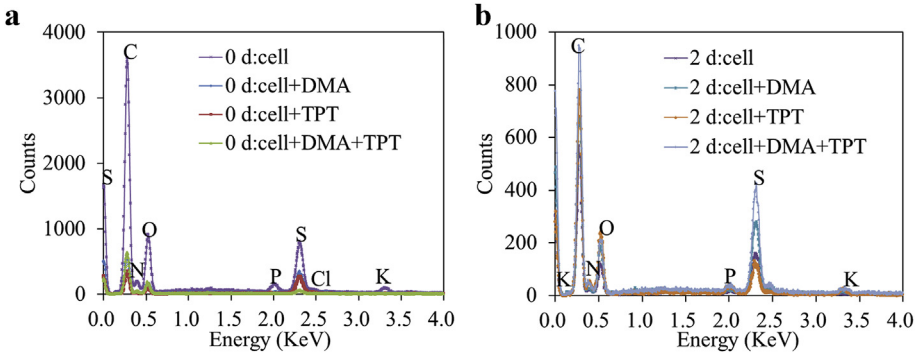

Fig. 3. Cell surface element analysis. a: samples treated for 0 d; b: samples treated for 2 d.

medium with TPT or DMA recovered to some degree after 2 d (Fig. 3b) because these molecules act as nutrients. Nevertheless, element metabolism of the control cells decreased after 2 d (Fig. 3b) compared with the other three samples, which was due to nutrient deficiency.

3.4. FA analysis

To analyze the interaction between membrane structure, composition, cellular metabolism and TPT transport, FAs were detected in the current study. Except for unsaturated omega-9 Fas (Fig. 4d, palmitoleic acid, PAA, C16:1n−9; Fig. 4h, oleic acid, OA, C18:1n−9) and omega-6 FA (Fig. 4g, linoleic acid, LA, C18:2n−6), five of them were long-chain saturated FAs, including myristic acid (MA, Fig. 4b, C14:0), pentadecanoic acid (PEA, Fig. 4c, C15:0), palmitic acid (PA, Fig. 4e, C16:0), heptadecanoic acid (HA, Fig. 4f, C17:0) and stearic acid (SA, Fig. 4i, C18:0). PA (Fig. 4e, up to 42,468 mg kg^{-1}) and SA (Fig. 4i, up to 16,186 mg kg^{-1}) were the two major FAs among them. The composition of different FAs in the cellular membrane is directly related to membrane fluidity, cellular signal transduction, cell adhesion, proliferation and survival. Polyunsaturated FA levels in normal cells were low and almost undetectable because they inhibited enzyme metabolism involved in drug and xenobiotic transformation (Yao et al., 2006). There were no such FAs detected in the current samples, which indicates that *B. thuringiensis* survived well even though suffering from starvation or the toxicity of TPT and its metabolites for 7 d.

FAs modulated cellular responses, which were essential to glucose homeostasis, and played a significant role as energy substrates for cells (Rodrigues et al., 2016). In general, the results of Fig. 4b–i were opposite to those of Fig. 4a. FAs would increase under stresses when biomass decrease, which was the main reason that FAs were biomarkers indicating the response of microbes to environmental changes (Yao et al., 2015). The current finding also illustrates that the inhibitory influence of starvation on cells was more severe than that of TPT toxicity, which was consistent with the results of Fig. 3. TPT with DMA significantly depressed MA, LA and SA production, which indicates that cells in the medium with TPT and DMA were more active than in other treatments. Fig. 4e and h shows the significant effect of TPT on FA synthesis. It has been reported that both PA and OA could modulate the production of reactive oxygen compounds resulting in cell oxidative damage and even inducing the apoptosis of some cells (Carrillo et al., 2011; Guerra and Otton, 2011; Hidalgo et al., 2011), which illustrates that TPT had a detrimental effect on cells by changing the concentrations or species of FAs. Although the biomass under TPT stress in the MSM significantly decreased (Figs. 2 and 4a), approximately 50% of the cells were still viable. This finding suggests that the cytoplasm released by cells after apoptosis was used by viable cells. In the meantime, the permeability-enhancing effect of PA and OA helped cells to utilize extracellular nutrients by the generation of transient pores to maintain mass balance (Arouri and Mouritsen, 2013). Nevertheless, the unfavorable elastic tension formed during the pore formation process could ultimately cause pore disintegration (Teixeira et al., 2012) resulting in cell mass decrease in the samples without TPT. Fig. 4b, g and i exhibit the positive influence of DMA on the membrane under TPT stress. SA could also trigger the production of reactive oxygen species (Guerra and Otton, 2011). The metabolite of LA in bacterial cells was 10-oxo-12(Z)-octadecenoic acid, which increased adiponectin production, glucose uptake and energy metabolism by regulating the activity of peroxisome proliferator-activated receptors (Goto et al., 2015). The low LA concentration in the medium containing TPT and DMA indicates that cells produced more 10-oxo-12(Z)-octadecenoic acid and energy. The energy generated by DMA assimilation in this condition could be used to enhance TPT transport and degradation, which was consistent with the results of Fig. 1b. MA in the proper concentrations led to an increasing expression of peroxisome proliferator activated receptor, mRNA and adipose-related genes, like glucose transporter, FA binding protein, FA translocase, acetyl-CoA carboxylase and FA synthase (Huang et al., 2012; Puhl et al., 2012). Specifically, MA promoted the glycolysis, influenced FA transport and FA de novo synthesis, and increased the content of saturated FAs (Lu et al., 2014). Thus, the content of SA and LA could be influenced by MA.

FAs are composed of an aliphatic chain and a carboxylic acid moiety. Their synthesis is regulated by acetyl-CoA or malonyl-CoA, which then converts into acetyl-[acyl-carrier-protein] (acp) and malonyl-acp. The enzymes involved in this process include acetyl-CoA carboxylase, malonyl CoA-acyl carrier protein transacylase, 3-oxoacyl-acp synthase, 3-oxoacyl-acpreductase, 3-hydroxyacyl-acpdehydratase, enoyl-acpreductase and acyl-acp-hydrolase (http://www.kegg.jp/kegg-bin/highlight_pathway?scale=1.0&map=btb01212). The majority of the myristoyl-acps reacted with malonyl-acp to successively form hexadecanoyl-acp, palmitoyl-acp and PA. The same enzymes also participated in the synthesis of different FAs. Hence, a high PA concentration in cells was due to high substrate concentrations. Among these carrier proteins, hexadecanoyl-acp transformed to stearoyl-acp, stearic-acp and SA, sequentially. Except for the formation of SA with a mass ranking second in the current study, stearoyl-acp also converted into oleoyl-acp and then OA. The generated oleoyl-acp further formed linoleoyl-acp and LA. Compared with PA synthesis, only a minority of myristoyl-acps reacted with acetyl-acp to form PEA, and small amounts of hexadecanoyl-acp formed PAA and HA.

A FA chain forms one 1-acyl-sn-glycerol-3-phosphate (ASGP) and generates phosphatidic acid (1,2-diacyl-sn-glycerol-3-phosphate, DSGP) for further reaction with acyl-CoA by ASGP acyltransferase (EC 2.3.1.51) (Equation (1)). In addition, two FA chains interact with one ethyl alcohol to produce 1,2-diacyl-sn-glycerol (DSG) and subsequently combine with PO_4^{3-} to form DSGP under the catalysis of diacylglycerol kinase (EC2.7.1.107) (Equation (2)). Finally, DSGP interacts with some special groups (such as choline) under catalysis of alkaline phosphatase (EC 3.1.3.1) to generate membrane structure compounds such as phosphatidylcholine (Equation (3)). The FA content of cells in MSM without TPT was in general higher, which means that the above-mentioned compounds were higher as well. ASGP is related to absorption and degradation of lipids and vitamins. Fat degradation caused biomass decrease due to starvation (Fig. 4a), while TPT was assimilated as a nutrient by the cells. Fig. 5b and c shows that TPT enlarged membrane permeability accelerating transport. Moreover, vitamins are tightly bound to enzymes serving as part of prosthetic groups. Biotin for example, as part of enzymes involved in FAs synthesis, conversely formed FAs to increase FA content in the samples without TPT (Bolander, 2006). DSG was connected to inositol phosphate metabolism and also involved in fat breakdown, cell growth and apoptosis (Cario et al., 2015). The phosphorylation compound DSGP plays an important role for cAMP-dependent pathway (http://www.kegg.jp/kegg-bin/show_pathway?map04024+C00416). cAMP can lead to the activation of cyclic nucleotide-gated ion channels transporting Ca^{2+} or Na^{+} into cells and phosphorylating an enzyme that converts glycogen into glucose. Therefore, DSGP accumulation in the medium without TPT resulted in the decrease of MP by depolarization. Apart from acyl-acp-hydrolase, all of the other proteins were found in *B.*

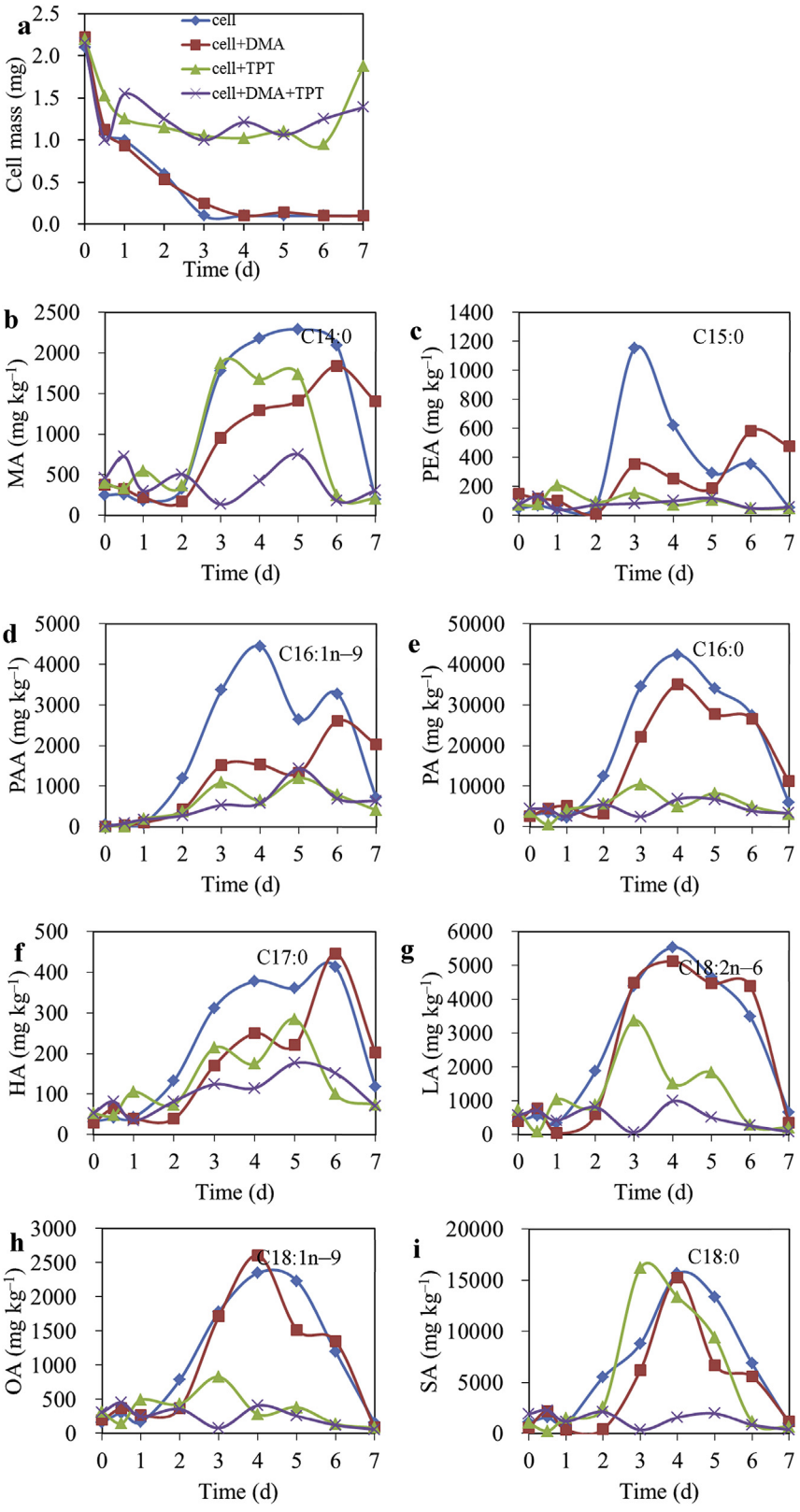

Fig. 4. The change of cell mass and FAs with time.

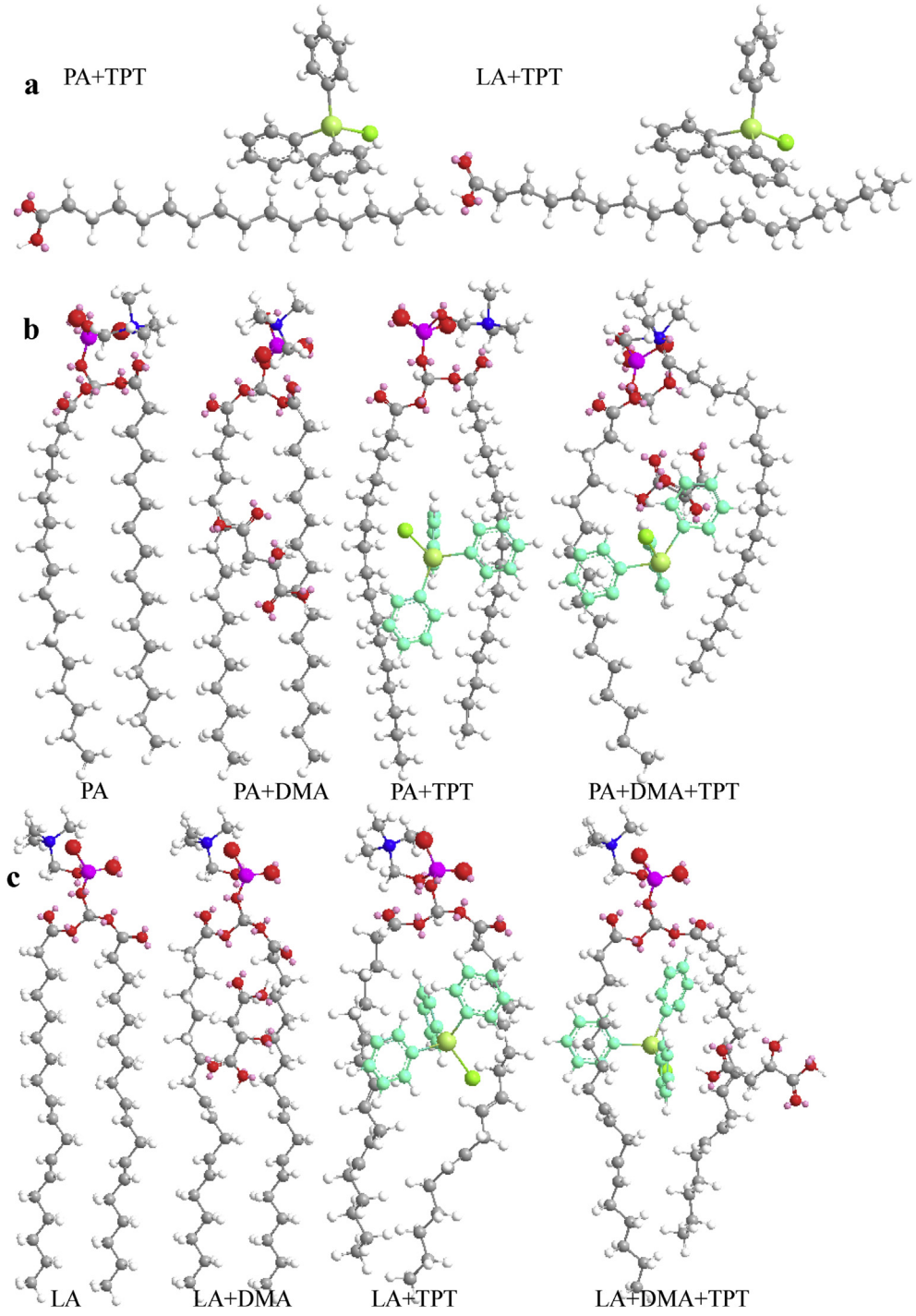

Fig. 5. The interactions among FAs, TPT and DMA.

thuringiensis by genome sequencing, which demonstrates the veracity of the FA synthesis pathway and phospholipid metabolism.

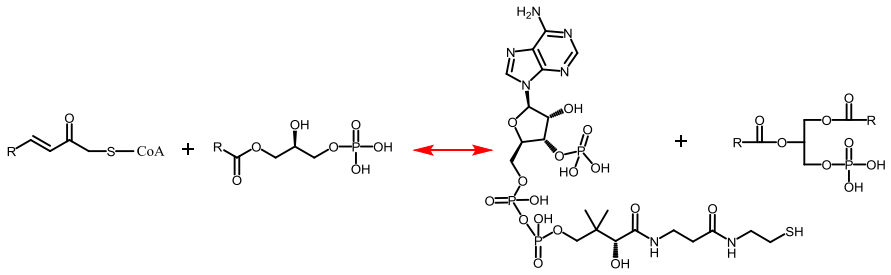

(1)

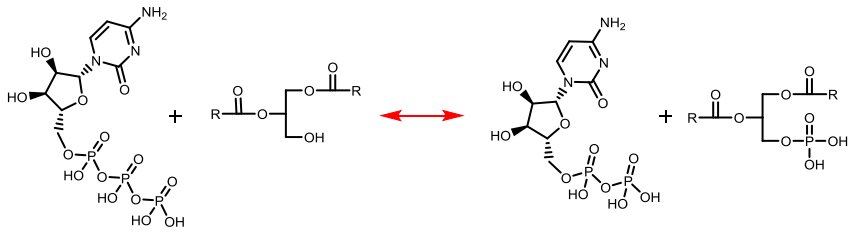

(2)

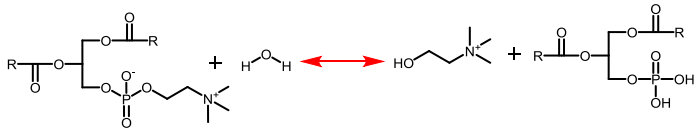

(3)

Although the existence of double bonds in a FA chain varied the structure (Fig. 5a), there was no significant difference in distances between FAs and TPT when they were in a stable state (Table S1). In addition, there was no significant difference in TPT bond energy under varying conditions (Table S2). Fig. 5b and c shows that TPT or the mixture of DMA and TPT enhanced membrane permeability, which was another reason for the recovery of element metabolism in the samples with TPT or DMA (Fig. 3b). For example, the distance between two LA chains increased from 6.5 Å to approximately 13 Å in the presence of TPT with or without DMA (Fig. 5c). The combination of DMA and TPT significantly altered the topological structure of PA (Fig. 5b) compared with LA (Fig. 5c). Therefore, TPT or the mixture of DMA and TPT not only was used as nutrients and reduced FA synthesis but also increased membrane permeability, thus accelerating material transport.

3.5. MP analysis

The results of FAs reveal that the structure and composition of the membrane (Figs. 4 and 5) would change under the stress of pollutants or starvation, which certainly affected microbial metabolism and the interaction with pollutants (Fig. 2). Ion selection by ion transporters results in unbalanced ion distribution between inside (negative charge) and outside (positive charge) of the cell membrane and forms a potential difference, which is called MP. This difference is related to signal transduction, ATPase and proton pump activities. It will change when cells are under stresses. If the alteration goes beyond a certain range, the cell functions would be damaged (David et al., 2012).

JC−1 is a lipophilic cationic fluorescent dye, which forms red fluorescence-emitting J-aggregates when MP is high and forms green-emitting JC−1 monomers in the opposite condition. The results shown in Fig. 6a were consistent with those in Fig. 4a, which reveals the accuracy of this method for *B. thuringiensis*. The initially decreasing MP (Fig. 6a) was due to the change of membrane structure and composition, triggering by TPT toxicity or starvation (Figs. 4 and 5). The ANOVA results show that the effect of DMA on MP was limited because DMA in the medium was used fast and DMA did not have a significant inhibitory influence on cells. The similar effect of TPT illustrates that TPT altered cellular elements, FA composition and membrane structure but it only had limited influence on MP. The combination of TPT and DMA significantly relieved MP decrease, which was one reason that DMA promoted TPT degradation (Fig. 1b).

The change in MP would influence H^+-ATP synthase serving as a core hub in energy metabolism and cell death regulation (Martínez-Reyes and Cuezva, 2014; Lee et al., 2016; Silvestri et al., 2016), which both significantly affected cell metabolism and TPT biodegradation. The excess H^+ provided by DMA in high concentration (Fig. 2a) inhibited the transfer of intracellular H^+ to the periplasm leading to low MP and further inhibiting other cellular metabolisms, which was another reason for low TPT degradation rate in the meantime.

It has been observed from CLSM that red and green fluorescence

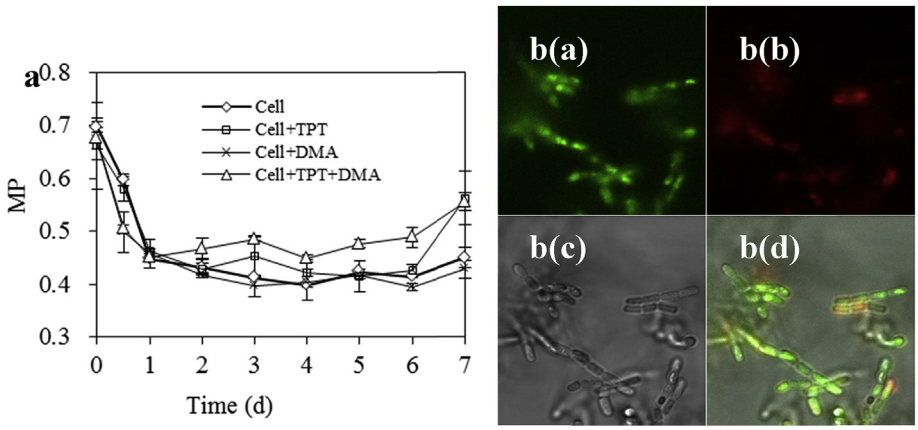

Fig. 6. MP analysis. a: MP change with time; b: JC−1 fluorescence analysis, (a): green fluorescence reflecting the monomeric state of JC−1 within the cells; (b): red fluorescence reflecting JC−1 aggregation within the cells; (c): cells shown without fluorescence; (d): cells shown with red and green fluorescence. (For interpretation of the references to colour in this figure legend, the reader is referred to the web version of this article.)

intensity would change with the addition of TPT or DMA. However, fluorescence-emitting areas all focused on endospores (Fig. 6b). This finding means that endospores could serve as an index to evaluate the cellular physiological and biochemical situation. The spore wall has three layers, including an outer protein shell, a middle peptidoglycan cortex containing a large number of 2,6-pyridine dicarboxylic acids, and a peptidoglycan lining. When the spore wall is integrated, JC−1 forms red fluorescence-emitting J-aggregates in the spore wall. However, JC−1 forms green-emitting JC−1 monomers in the spore cytoplasm when the spore wall is damaged. This method could therefore not only be used to evaluate cellular activity but also served as a new way to reveal the state of endospores.

4. Conclusions

The assimilation of DMA at concentrations of 0.5 and 1 mg L^{-1} could dramatically promote TPT biodegradation to approximately 90% by regulating H^+ metabolism, cellular element metabolism, FA synthesis, membrane permeability, membrane structure and spore activity. The main FAs synthesized by *B. thuringiensis* were PA and SA. Although they could induce the production of reactive oxygen compounds, their proper increase could enlarge transient pores and stimulate the assimilation of extracellular carbon source. In addition, the interaction between TPT and FAs could also enhance membrane permeability directly. TPT with DMA significantly depressed MA, LA and SA production, while TPT alone notably reduced PA and OA, which means that TPT and DMA were beneficial to cellular survival compared to starvation. Endospores could act as an indicator for MP and cellular activities through fluorescence analysis.

Acknowledgements

The authors would like to thank the National Natural Science Foundation of China (Nos. 21377047, 21577049), Science and Technology Project of Guangdong Province (Nos. 2014A020216013, 2016A020222005) and the University Foundation of Education Ministry of China (No. 21615459) for their financial support.

Appendix A. Supplementary data

Supplementary data related to this article can be found at http://dx.doi.org/10.1016/j.chemosphere.2016.10.140.

References

Arouri, A., Mouritsen, O.G., 2013. Membrane-perturbing effect of fatty acids and lysolipids. Prog. Lipid Res. 52, 130–140.
Bernat, P., Dlugonski, J., 2012. Comparative study of fatty acids composition during cortexolone hydroxylation and tributyltin chloride (TBT) degradation in the filamentous fungus *Cunninghamella elegans*. Int. Biodeterior. Biodegrad. 74, 1–6.
Bolander, F.F., 2006. Vitamins: not just for enzymes. Curr. Opin. Investig. Drugs 7, 912–915.
Cario, A., Mizgier, A., Thiel, A., Jebbar, M., Oger, P.M., 2015. Restoration of the di-myo-inositol-phosphate pathway in the piezo-hyperthermophilic archaeon *Thermococcus barophilus*. Biochimie 118, 286–293.
Carrillo, C., del Mar-Cavia, M., Roelofs, H., Wanten, G., Alonso-Torre, S.R., 2011. Activation of human neutrophils by oleic acid involves the production of reactive oxygen species and a rise in cytosolic calcium concentration: a comparison with N-6 polyunsaturated fatty acids. Cell. Physiol. Biochem. 28, 329–338.
Clarke, B.O., Smith, S.R., 2011. Review of 'emerging' organic contaminants in biosolids and assessment of international research priorities for the agricultural use of biosolids. Environ. Int. 37, 226–247.
Cole, R.F., Mills, G.A., Parker, R., Bolam, T., Birchenough, A., Kröger, S., Fones, G.R., 2015. Trends in the analysis and monitoring of organotins in the aquatic environment. Trends Anal. Chem. 8, 1–11.
David, F., Hebeisen, M., Schade, G., Franco-Lara, E., di Berardino, M., 2012. Viability and membrane potential analysis of *Bacillus megaterium* cells by impedance flow cytometry. Biotechnol. Bioeng. 109, 483–492.
dos Santos, M.M., Raghevendrana, V., Kotterb, P., Olssona, L., Nielsen, J., 2004. Manipulation of malic enzyme in *Saccharomyces cerevisiae* for increasing NADPH production capacity aerobically in different cellular compartments. Metab. Eng. 6, 352–363.
Fickova, M., Macho, L., Brtko, J., 2015. A comparison of the effects of tributyltin chloride and triphenyltin chloride on cell proliferation, proapoptotic p53, Bax, and antiapoptotic Bcl-2 protein levels in human breast cancer MCF-7 cell line. Toxicol. Vitro 29, 727–731.
Fortibuoni, T., Noventa, S., Rampazzo, F., Gion, C., Formalewicz, M., Berto, D., Raicevich, S., 2013. Evidence of butyltin biomagnification along the Northern Adriatic food-web (Mediterranean Sea) elucidated by stable isotope ratios. Environ. Sci. Technol. 47, 3370–3377.
Fostera, A., Barnesb, N., Speightb, R., Keanea, M.A., 2013. Genomic organisation, activity and distribution analysis of themicrobial putrescine oxidase degradation pathway. Syst. Appl. Microbiol. 36, 457–466.
Goto, T., Kim, Y.I., Furuzono, T., Takahashi, N., Yamakuni, K., Yang, H.E., Li, Y.J., Ohue, R., Nomura, W., Sugawara, T., Yu, R., Kitamura, N., Park, S.B., Kishino, S., Ogawa, J., Kawada, T., 2015. 10-oxo-12(Z)-octadecenoic acid, a linoleic acid metabolite produced by gut lactic acid bacteria, potently activates PPARg and stimulates adipogenesis. Biochem. Biophys. Res. Commun. 459, 597–603.
Graceli, J.B., Sena, G.C., Lopes, P.F.I., Zamprogno, G.C., Costa, M.B.D., Godoi, A.F.L., Santos, D.M.D., Marchi, M.R.R.D., Fernandez, M.A.D.S., 2013. Organotins: a review of their reproductive toxicity, biochemistry, and environmental fate. Reprod. Toxicol. 36, 40–52.
Guerra, B.A., Otton, R., 2011. Impact of the carotenoid astaxanthin on phagocytic capacity and ROS/RNS production of human neutrophils treated with free fatty acids and high glucose. Int. Immunopharmacol. 11, 2220–2226.
Gui, W., Tian, C., Sun, Q., Li, S., Zhang, W., Tang, J., Zhu, G., 2016. Simultaneous determination of organotin pesticides by HPLC–ICP–MS and their sorption, desorption, and transformation in freshwater sediments. Water Res. http://dx.doi.org/10.1016/j.watres.2016.02.056.

Hidalgo, M.A., Nahuelpan, C., Manosalva, C., Jara, E., Carretta, M.D., Conejeros, I., Loaiza, A., Chihuailaf, R., Burgos, R.A., 2011. Oleic acid induces intracellular calcium mobilization, MAPK phosphorylation, superoxide production and granule release in bovine neutrophils. Biochem. Biophys. Res. Commun. 409, 280–286.

Huang, J., Ye, J.S., Ma, J.W., Gao, J., Chen, S.Q., Wu, X.L., 2014. Triphenyltin biosorption, dephenylation pathway and cellular responses during triphenyltin biodegradation by *Bacillus thuringiensis* and tea saponin. Chem. Eng. J. 249, 167–173.

Huang, X.F., Li, M.X., Lu, L.J., Yang, S., Liu, J., 2012. Relationship of cell-wall bound fatty acids and the demulsification efficiency of demulsifying bacteria *Alcaligenes* sp. S-XJ-1 cultured with vegetable oils. Bioresour. Technol. 104, 530–536.

Kostudis, S., Bachmann, K., Kutschke, S., Pollmann, K., Gutzmer, J., 2015. Leaching of copper from Kupferschiefer by glutamic acid and heterotrophic bacteria. Min. Eng. 75, 38–44.

Lee, D.G., Choi, B.K., Kim, Y.H., Oh, H.S., Park, S.H., Bae, Y.S., Kwon, B.S., 2016. The repopulating cancer cells in melanoma are characterized by increased mitochondrial membrane potential. Cancer Lett. 382, 186–194.

Lu, N.S., Shu, G., Xie, Q.P., Zhu, X.T., Gao, P., Zhou, G.X., Wang, S.B., Wang, L.N., Xi, Q.Y., Zhang, Y.L., Jiang, Q.Y., 2014. Myristic acid (MA) promotes adipogenic gene expression and the differentiation of porcine intramuscular adipocyte precursor cells. J. Integr. Agric. 13, 2488–2499.

Martínez-Reyes, I., Cuezva, J.M., 2014. The H^+-ATP synthase: a gate to ROS-mediated cell death or cell survival. Biochim. Biophys. Acta 1837, 1099–1112.

Niu, J., Homan, T.G., Arentshorst, M., de Vries, R.P., Visser, J., Ram, A.F.J., 2015. The interaction of induction and repression mechanisms in the regulation of galacturonic acid-induced genes in *Aspergillus Niger*. Fungal Genet. Biol. 82, 32–42.

Podratz, P.L., Merlo, E., Sena, G.C., Morozesk, M., Bonomo, M.M., Matsumoto, S.T., da Costa, M.B., Zamprogno, G.C., Brandão, P.A.A., Carneiro, M.T.W.D., Miguel, E.D.C., Miranda-Alves, L., Silva, I.V., Graceli, J.B., 2015. Accumulation of organotins in seafood leads to reproductive tract abnormalities in female rats. Reprod. Toxicol. 57, 29–42.

Puhl, A.C., Bernardes, A., Silveira, R.L., Yuan, J., Campos, J.L., Saidemberg, D.M., Palma, M.S., Cvoro, A., Ayers, S.D., Webb, P., Reinach, P.S., Skaf, M.S., Polikarpov, I., 2012. Mode of peroxisome proliferator-activated receptor γ activation by luteolin. Mol. Pharmacol. 81, 788–799.

Rodrigues, H.G., Sato, F.T., Curi, R., Vinolo, M.A.R., 2016. Fatty acids as modulators of neutrophil recruitment, function and survival. Eur. J. Pharmacol. 785, 50–58.

Silvestri, S., Orlando, P., Brugè, F., Falcioni, G., Tiano, L., 2016. Effect of different metals on oxidative state and mitochondrial membrane potential in trout erythrocytes. Ecotox. Environ. Safe 134, 280–285.

Tang, L.T., Wang, L.L., Ou, H.S., Li, Q.S., Ye, J.S., Yin, H., 2016. Correlation among phenyltins molecular properties, degradation and cellular influences on *Bacillus thuringiensis*in the presence of biosurfactant. Biochem. Eng. J. 105, 71–79.

Teixeira, V., Feio, M.J., Bastos, M., 2012. Role of lipids in the interaction of antimicrobial peptides with membranes. Prog. Lipid Res. 51, 149–177.

Wang, L.L., Tang, L.T., Wang, R., Wang, X.Y., Ye, J.S., Long, Y., 2016. Biosorption and degradation of decabromodiphenyl ether by *Brevibacillus brevis* and the influence of decabromodiphenyl ether on cellular metabolic responses. Environ. Sci. Pollut. R. 23, 5166–5178.

Yao, H.T., Chang, Y.W., Lan, S.J., Chen, C.T., Hsu, J.T.A., Yeh, T.K., 2006. The inhibitory effect of polyunsaturated fatty acids on human CYP enzymes. Life Sci. 79, 2432–2440.

Yao, H.Y., Chapman, S.J., Thornton, B., Paterson, E., 2015. ^{13}C PLFAs: a key to open the soil microbial black box? Plant Soil 392, 3–15.

Ye, J.S., Yin, H., Peng, H., Bai, J.Q., Xie, D.P., Wang, L.L., 2013. Biosorption and biodegradation of triphenyltin by *Brevibacillus brevis*. Bioresour. Technol. 129, 236–241.

Zdravkovic, I., Zhao, C.F., Lev, B., Cuervo, J.E., Noskov, S.Y., 2012. Atomistic models of ion and solute transport by the sodium-dependent secondary active transporters. Biochim. Biophys. Acta 1818, 337–347.